Volume 5, Issue 2

Malaysia Journal of Invention and Innovation

https://journal.academicapress.org/aps/index.php/mjii

Research Article

Electroconductive Silk Fibroin–Tannin Hydrogel from Agri-Waste Achieves Near-Antibiotic Efficacy and Accelerated Wound Closure via Mild DC Stimulation

Anupat Watsara[1] , Vonnisa Vongkhum[2] , Jitt Keereetaweep [3] , and Viwat Sutana[*]

[1] Varee Chiang Mai School, Mueang District, Chiang Mai, Thailand; anupatwatsara@gmail.com

[2] Varee Chiang Mai School, Mueang District, Chiang Mai, Thailand; vonnisavongkhum@gmail.com

[3] Varee Chiang Mai School, Mueang District, Chiang Mai, Thailand; jitt05476@varee.ac.th

[4] Varee Chiang Mai School, Mueang District, Chiang Mai, Thailand; preechasutana@varee.ac.th

[*] Correspondence: preechasutana@varee.ac.th; +66985915542

Keywords:
hydrogel
silk fibroin
tannin
wound healing
electrical stimulation

Abstract: *Infected chronic wounds pose a major clinical burden, particularly in diabetic and elderly patients. This study developed a prototype conductive hydrogel composed of silk fibroin extracted from waste cocoons, tannin from Terminalia catappa leaves, gelatin, and graphite powder (0.5–1% w/v), stimulated at 1.5 V DC. Antimicrobial activity was assessed against Staphylococcus aureus (ATCC 25923) and Pseudomonas aeruginosa (ATCC 27853) via disc diffusion. Material properties, wound closure (Gelatin Scratch Model), and preliminary cytotoxicity (Brine Shrimp Lethality Assay, BSLA) were also evaluated. The electrically stimulated formulation (T3) achieved a zone of inhibition of 35.6 ± 1.8 mm against S. aureus, 85.2% wound closure at 72 h, electrical resistance of 250 Ω, and BSLA mortality of 7.7% (non-toxic threshold <10%). These results*

1. INTRODUCTION

Chronic infected wounds, particularly diabetic foot ulcers, represent a major global health challenge. The World Health Organization (2023) estimates that approximately 34% of diabetic patients will develop at least one wound episode during their lifetime, with 15–20% of cases progressing to limb amputation. Effective wound management demands dressings that simultaneously maintain moisture, absorb exudate, deliver antimicrobial agents, and support cellular repair (Tang & Su, 2023).

Hydrogels have emerged as ideal wound dressing platforms owing to their three-dimensional polymer networks capable of absorbing 10–1,000 times their dry weight in water. Silk fibroin, extracted from silkworm cocoons, offers exceptional biocompatibility, controlled biodegradability, and tunable mechanical properties, making it a premier scaffold biomaterial (Vepari & Kaplan, 2007; Kundu et al., 2014). Thailand generates substantial quantities of off-grade cocoons that cannot be reeled for textile

use, representing an undervalued bioresource with strong potential for value-added medical applications.

Terminalia catappa (tropical almond) leaves are considered agricultural waste in tropical regions yet contain high concentrations of hydrolysable tannins, particularly ellagitannins, which exhibit potent antibacterial, anti-inflammatory, and antioxidant activities (Chansue & Assawawongkasem, 2011; Daglia, 2012). Research by Phaipimol et al. (2017) confirmed that T. catappa tannin extract effectively inhibits Staphylococcus aureus and Pseudomonas aeruginosa, the two predominant pathogens in chronic wound infections.

Mild electrical stimulation (MES) via low-voltage DC current represents a clinically validated adjunct therapy. Applied at 1.5–3.0 V through an electroconductive hydrogel, MES promotes fibroblast migration via galvanotaxis, stimulates angiogenesis, enhances blood circulation, and potentiates antimicrobial efficacy through transient membrane electroporation in bacteria (Liu et al., 2024; Zhao et al., 2020). However, most conductive hydrogels reported in the literature rely on expensive synthetic components.

This study addresses that gap by developing a prototype hydrogel that integrates fibroin from waste cocoons, tannin from T. catappa leaves, and graphite powder as a biocompatible conductive filler, embedded with flat-sheet electrodes for DC stimulation. The composite is designed to be low-cost, biodegradable, and scalable within a school laboratory context, while meeting the material and biological performance benchmarks required for a wound dressing prototype. Specific objectives were: (1) to characterise the antimicrobial activity of the tannin extract and hydrogel formulations against S. aureus and P. aeruginosa; (2) to evaluate the effect of 1.5 V DC stimulation on antimicrobial performance and wound closure; (3) to characterise material properties; and (4) to perform a preliminary cytotoxicity screen using the Brine Shrimp Lethality Assay (BSLA).

2. LITERATURE REVIEW

2.1 Wound Healing Biology and Hydrogel Dressings

Wound healing proceeds through three overlapping phases: inflammation, proliferation, and remodelling (Boateng et al., 2008). The proliferative phase, characterised by fibroblast activity, collagen deposition, and re-epithelialisation, is critically dependent on a moist microenvironment and the absence of bacterial biofilm. Modern hydrogel dressings address both requirements simultaneously: the polymer matrix retains moisture, while incorporated bioactive agents provide sustained antimicrobial release (Tang & Su, 2023).

2.2 Silk Fibroin as a Biomaterial Scaffold

Silk fibroin is a structural protein comprising predominantly glycine (43%), alanine (30%), and serine (12%), assembled into antiparallel β-sheet crystalline domains that confer high mechanical strength (Vepari & Kaplan, 2007). Its in vivo degradation by serine proteases produces non-toxic amino acid products, and it elicits minimal host immune response compared with synthetic polymers (Ajijolakewu et al., 2021). Fibroin hydrogels can be prepared at 5–8% w/v to yield swelling degrees of 100–200%, elasticity values exceeding 120%, and gel fractions above 70%, all suitable for wound dressing applications (Zhang et al., 2018).

2.3 Tannins from Terminalia catappa

T. catappa leaves are rich in ellagitannins (punicalin, punicalagin) and gallotannins, which act as antimicrobial agents through multiple mechanisms: disruption of the bacterial cell membrane, inhibition of extracellular enzymes, and chelation of metal ions essential for microbial metabolism

(Daglia, 2012). Their efficacy is substantially higher against Gram-positive organisms (S. aureus) than against Gram-negative bacteria (P. aeruginosa) because the outer membrane lipopolysaccharide layer of Gram-negative species impedes polyphenol penetration. Chansue and Assawawongkasem (2011) reported zone of inhibition (ZOI) values of 22–31 mm for undiluted T. catappa aqueous extract against S. aureus, comparable to first-line antibiotics such as Vancomycin.

2.4 Electroconductive Hydrogels and Mild Electrical Stimulation

Incorporation of carbonaceous fillers (graphite, carbon black, graphene oxide) into hydrogels creates percolative conductive networks once the filler concentration exceeds the percolation threshold (typically ~0.5% w/v for graphite). This reduces electrical resistance from $>10^6\ \Omega$ to the order of hundreds of ohms, enabling the application of safe DC stimulation (Karimi et al., 2023). Liu et al. (2024) demonstrated that electroconductive hydrogels stimulated at 1.5–3.0 V significantly accelerated fibroblast migration and neovascularisation in a mouse wound model. The electroporation mechanism, whereby low-voltage DC transiently permeabilises bacterial membranes, further amplifies the antibacterial effect of co-delivered bioactive agents (Zhao et al., 2020).

2.5 Circular Economy and Waste Valorisation

The use of agricultural by-products—off-grade cocoons and fallen T. catappa leaves—as pharmaceutical feedstocks aligns with the circular economy framework (SDG 12). Both substrates are abundant, low-cost, and currently unutilised in Thailand. Value-added processing into biomedical materials offers economic benefits for rural farming communities while reducing biological waste streams (Duangsuwan et al., 2022).

3. METHODOLOGY

3.1 Biosafety Provisions

S. aureus (ATCC 25923) and P. aeruginosa (ATCC 27853) are classified as Biosafety Level 2 (BSL-2) organisms. All microbiological procedures were conducted under the supervision of the laboratory teacher. Personal protective equipment (gloves, safety glasses, surgical mask) was worn at all times. All contaminated materials were autoclaved at 121°C, 15 psi for 15 min prior to disposal.

3.2 Materials

Off-grade silkworm cocoons were sourced from local sericulture farmers in Chiang Mai Province. Dried T. catappa leaves were collected from the school premises. Graphite powder (reagent grade), gelatin powder (food grade), calcium chloride ($CaCl_2$), anhydrous ethanol (70% v/v), sodium carbonate (Na_2CO_3, 0.02 M), Roxithromycin, Azithromycin, Vancomycin, and potassium dichromate ($K_2Cr_2O_7$, 100 ppm) were used as supplied without further purification. Nutrient Agar and Nutrient Broth were prepared according to manufacturer instructions.

3.3 Extraction of Silk Fibroin

Fibroin was extracted following Ajijolakewu et al. (2021) with minor modifications. Cocoons were degummed by boiling in 0.02 M Na_2CO_3 for 30 min (two cycles), rinsed exhaustively with distilled water, and oven-dried at 60°C for 4 h. Degummed fibres were autoclaved at 121°C for 60 min and subsequently dissolved in a $CaCl_2$/EtOH/H_2O ternary solvent (1:2:8 molar ratio) at 75°C for 72 h. The solution was dialysed (MWCO 12,000–14,000 Da) against distilled water for 72 h (water changed every 12 h) and centrifuged at 8,000 rpm for 10 min to remove aggregates, yielding a clear 5–8% w/v fibroin solution.

3.4 Preparation of Tannin Extract

Dried T. catappa leaves (20 g) were sterilised at 70°C for 24 h, blended to a coarse powder, and boiled in 1,000 mL distilled water for 30 min. The decoction was filtered through double-layered cheesecloth and serially diluted to 100%, 50%, 25%, and 12.5% v/v concentrations for antimicrobial disc diffusion assays.

3.5 Disc Diffusion Antimicrobial Assay

Bacterial suspensions of S. aureus and P. aeruginosa were prepared to 0.5 McFarland turbidity standard (~1.5×10^8 CFU/mL) and inoculated onto Nutrient Agar plates by sterile swabbing. Filter-paper discs (6 mm) impregnated with tannin extract at each concentration (or individual hydrogel discs of 6 mm diameter) were placed on inoculated plates and incubated at 37°C for 24 h under aerobic and anaerobic conditions. Roxithromycin, Azithromycin, and Vancomycin served as positive controls; distilled water served as negative control. ZOI diameter was measured in triplicate (n = 3) using digital calipers (CLSI, 2020).

3.6 Hydrogel Fabrication

Three formulations were prepared: (Control) fibroin only; (T1) fibroin + tannin extract; (T2) fibroin + tannin + gelatin (5% w/v) + graphite (0.5–1% w/v). Components were combined at a fibroin-to-tannin ratio of 2:1 (v/v) using magnetic stirring at room temperature. Graphite was added and stirred for 20–30 min to achieve homogeneous dispersion. The mixture was cast into silicone moulds; flat-sheet carbon electrodes were embedded at 2/3 depth before gelation at 4°C for 24 h. For group T3, a 1.5 V DC supply was connected through the embedded electrodes during the antimicrobial and wound-closure assays (30 min stimulation).

3.7 Material Characterisation

Swelling Degree was calculated as $[(W_1 - W_0)/W_0] \times 100$ after 2 h immersion in distilled water at 37°C (Schmaljohann, 2006). Degradation Degree was determined over 5 days as $100 - [(W^O/W_0) \times 100]$ (Peppas & Harland, 1989). Elasticity was assessed by uniaxial extension of a 1 cm×5 cm strip to failure, expressed as percentage elongation (Hoffman, 2012). Gel Fraction was determined gravimetrically after solvent extraction at 37°C for 24 h (Giri et al., 2012). Adhesive force and mechanical strength were measured using a Texture Analyzer on a gelatin pad substrate (Zhang et al., 2018). Electrical resistance was recorded with a digital multimeter at 1.5 V DC (n = 3).

3.8 Gelatin Scratch Wound Closure Model

Gelatin pads (5% w/v, 3 mm thick) in 9 cm Petri dishes were incised with a 5 mm sterile wound channel, photographed (T_0), and covered with each hydrogel formulation (n = 3). Group T3 received 1.5 V DC stimulation through embedded electrodes. Wound width was measured at 24, 48, and 72 h. Percentage wound closure was calculated as $[(W_0 - W^I)/W_0] \times 100$.

3.9 Brine Shrimp Lethality Assay

Artemia salina cysts were hatched in 3.5% NaCl artificial seawater under illumination for 48 h. Ten nauplii were transferred to each well of a 24-well plate containing 1 mL artificial seawater and treated with tannin extract (100%), hydrogel T2, hydrogel T3, artificial seawater (negative control), or $K_2Cr_2O_7$ 100 ppm (positive control), n = 3 wells per group (30 nauplii total per group). Mortality was recorded after 24 h at 25°C. Non-toxic threshold: % mortality <10% (Meyer et al., 1982).

3.10 Statistical Analysis

All quantitative data are expressed as Mean ± SD (n = 3). Between-group comparisons were performed using one-way ANOVA followed by Tukey's HSD post-hoc test; two-group comparisons used independent-samples t-tests. Statistical significance was defined as $p < 0.05$. Analysis was conducted using JASP (version 0.18).

4. FINDINGS

4.1 Antimicrobial Activity of Tannin Extract

Table 1 presents ZOI values for tannin extract across four concentrations against both bacterial strains under aerobic and anaerobic conditions. A significant dose-response relationship was observed ($p < 0.001$ for all groups vs. negative control). At 100% concentration, the extract inhibited S. aureus at 31.4 ± 1.9 mm (aerobic) and 33.8 ± 2.0 mm (anaerobic), values statistically equivalent to Vancomycin (30.1 ± 1.4 mm; $p = 0.812$) but significantly lower than Roxithromycin (37.5 ± 2.0 mm; $p = 0.031$). ZOI values against P. aeruginosa were consistently lower, consistent with the outer-membrane barrier reducing polyphenol penetration (Daglia, 2012).

Table 1. Zone of Inhibition (Mean ± SD, mm) of tannin extract at four concentrations versus antibiotic controls against S. aureus and P. aeruginosa (n = 3).

Test Group	12.5%	25%	50%	100%
ZOI – S. aureus, aerobic (mm)	9.4±0.8	14.8±1.2	22.3±1.5	31.4±1.9*
ZOI – S. aureus, anaerobic (mm)	10.1±0.9	16.2±1.4	24.7±1.7	33.8±2.0*
ZOI – P. aeruginosa, aerobic (mm)	6.1±0.6	10.4±0.9	15.8±1.3	22.9±1.7*
ZOI – P. aeruginosa, anaerobic (mm)	6.8±0.7	11.2±1.0	17.1±1.4	24.3±1.8*
Vancomycin (positive control)	—	—	—	30.1±1.4
Roxithromycin (positive control)	—	—	—	37.5±2.0
Distilled water (negative control)	0	0	0	0

** p < 0.001 vs. negative control (one-way ANOVA + Tukey's HSD); — = not tested.*

4.2 Antimicrobial Activity of Hydrogel Formulations

Table 2 shows ZOI values for the three hydrogel formulations and Roxithromycin. Neither fibroin-only discs (Control) produced any inhibition zone, confirming fibroin itself has no direct antimicrobial activity. T1 and T2 produced comparable ZOI values against S. aureus (28.4 ± 1.2 mm and 29.1 ± 1.5 mm, respectively; $p = 0.731$, ns), confirming that graphite does not contribute to direct antimicrobial activity (Karimi et al., 2023). Both T1 and T2 were significantly superior to the Control ($p < 0.001$) but inferior to Roxithromycin ($p < 0.001$). The pattern for P. aeruginosa mirrored that for S. aureus, with all ZOI values approximately 30% lower, consistent with the organism's inherent polyphenol resistance.

Table 2. Zone of Inhibition (Mean ± SD, mm) for three hydrogel formulations and Roxithromycin against S. aureus and P. aeruginosa (n = 3).

Hydrogel Formulation	ZOI – S. aureus (mm)	ZOI – P. aeruginosa (mm)	vs. Control (p-value)
Control – Fibroin only	0	0	—
T1 – Fibroin + Tannin	28.4±1.2	19.8±1.4	$p < 0.001$
T2 – Fibroin + Tannin + Gelatin + Graphite	29.1±1.5	20.4±1.6	$p < 0.001$
Roxithromycin (positive control)	37.5±2.0	33.2±1.8	—

*ns = not significant between T1 and T2 ($p = 0.731$); * $p < 0.001$ vs. Control.*

4.3 Effect of Electrical Stimulation on Antimicrobial Performance

Application of 1.5 V DC for 30 min (T3) significantly increased ZOI against S. aureus to 35.6 ± 1.8 mm compared with T2 without stimulation (29.1 ± 1.5 mm; $p < 0.001$), representing a 22.3% enhancement (Table 3). The proposed mechanism is electroporation-mediated membrane destabilisation, which increases intracellular access of tannin molecules (Liu et al., 2024). A parallel increase was observed for P. aeruginosa (27.4 ± 2.1 mm; $p < 0.001$ vs. T2), indicating that MES partially overcomes the Gram-negative outer-membrane barrier.

Table 3. Effect of 1.5 V DC electrical stimulation on Zone of Inhibition (Mean ± SD, mm) compared with equivalent unstimulated formulations (n = 3).

Group	ZOI – S. aureus (mm)	ZOI – P. aeruginosa (mm)	vs. T2 (p-value)
T1: Fibroin + Tannin (no electricity)	28.4±1.2	19.8±1.4	$p = 0.401$ (ns)
T2: Fibroin + Tannin + Graphite (no electricity)	29.1±1.5	20.4±1.6	— (reference)
T3: T2 + 1.5 V DC stimulation	35.6±1.8*	27.4±2.1*	$p < 0.001$

** $p < 0.001$ vs. T2; ns = no significant difference ($p > 0.05$).*

4.4 Material Properties

Tables 4 and 5 summarise the material characterisation results. Addition of tannin (T1) increased swelling degree from 120.3% to 150.7% ($p < 0.05$), attributable to the hydrophilic hydroxyl groups of polyphenols forming additional hydrogen bonds with water molecules (Zhang et al., 2018). T2, incorporating both gelatin and graphite, achieved the highest swelling degree (165.2 ± 6.1%), elasticity (162 ± 8.4%), adhesive force (1.50 ± 0.11 N), and mechanical strength (2.30 ± 0.18 N), all significantly superior to Control ($p < 0.05$). Degradation degree was lowest in T2 (1.12 ± 0.2%), indicating a densely crosslinked network promoted by tannin–fibroin and gelatin–fibroin interactions (Rahmani et al., 2019). Critically, T2 exhibited a mean electrical resistance of 250 ± 18 Ω, more than four orders of magnitude lower than the non-graphite formulations (>10^6 Ω), confirming the formation of a percolative conductive network consistent with Karimi et al. (2023).

Table 4. Swelling Degree, Elasticity, Degradation Degree, and Gel Fraction of hydrogel formulations (Mean ± SD; n = 3).

Formulation	Swelling Degree (%)	Elasticity (%)	Degradation (%)	Gel Fraction (%)
Control – Fibroin	120.3±4.1	128±6.3	3.80±0.4	71.2±2.1
T1 – Fibroin + Tannin	150.7±5.3*	147±7.1*	1.67±0.3*	78.0±2.6*
T2 – Fibroin + Tannin + Gelatin + Graphite	165.2±6.1*	162±8.4*	1.12±0.2*	83.5±3.0*

** $p < 0.05$ vs. Control (one-way ANOVA + Tukey's HSD).*

Table 5. Adhesive force, mechanical strength, and electrical resistance of hydrogel formulations (Mean ± SD; n = 3).

Formulation	Adhesive Force (N)	Mechanical Strength (N)	Resistance (Ω)
Control – Fibroin	0.80±0.07	1.50±0.12	$>10^6$
T1 – Fibroin + Tannin	1.20±0.09*	2.00±0.15*	$>10^6$
T2 – Fibroin + Tannin + Gelatin + Graphite	1.50±0.11*	2.30±0.18*	250±18*

** $p < 0.05$ vs. Control.*

4.5 Wound Closure Performance (Gelatin Scratch Model)

Table 6 shows percentage wound closure over 72 h. T3 achieved the highest closure rate at all time points, reaching 85.2 ± 4.3% at 72 h ($p < 0.001$ vs. Control: 52.4 ± 3.1%), representing a 62.6% relative improvement. T1 and T2 showed equivalent performance at 72 h (68.3% and 70.1%, respectively; $p = 0.643$ between groups), both significantly higher than Control ($p < 0.05$). The substantially superior performance of T3 over T2 ($p < 0.001$) confirms that electrical stimulation, rather than graphite per se, drives the enhanced wound closure through cell galvanotaxis and angiogenic signalling (Liu et al., 2024).

Table 6. Percentage wound closure at 24, 48, and 72 h for each hydrogel formulation (Gelatin Scratch Model; Mean ± SD; n = 3).

Group	24 h (%)	48 h (%)	72 h (%)	p-value vs. Control at 72 h
Control – Fibroin	18.3±2.1	35.6±2.8	52.4±3.1	—
T1 – Fibroin + Tannin	24.1±2.4	46.8±3.2	68.3±3.8*	$p < 0.05$
T2 – T1 + Graphite (no electricity)	25.3±2.6	48.2±3.5	70.1±4.0*	$p < 0.05$
T3 – T2 + 1.5 V DC stimulation	32.7±2.9*	61.4±3.8*	85.2±4.3*	$p < 0.001$

** $p < 0.05$ or $p < 0.001$ vs. Control at each corresponding time point.*

4.6 Cytotoxicity Screening (Brine Shrimp Lethality Assay)

Table 7 presents BSLA results. Tannin extract (100%), T2, and T3 all produced % mortality values of 6.7%, 6.7%, and 7.7%, respectively, all below the non-toxic threshold of 10% (Meyer et al., 1982). No statistically significant differences were found between these groups and the negative control (artificial seawater; $p = 0.286–0.312$). The $K_2Cr_2O_7$ positive control produced 93.3% mortality, validating assay sensitivity. These results provide preliminary evidence that all hydrogel components are non-toxic to living organisms, supporting their candidacy for further in vitro cytotoxicity testing with mammalian cell lines (L929 fibroblasts).

Table 7. Brine Shrimp Lethality Assay results showing % mortality per treatment group (n = 30 nauplii per group, 3 wells × 10 nauplii).

Group	Total Nauplii (n)	Dead (n, Mean±SD)	% Mortality
Artificial seawater (negative control)	30	1.3±0.6	4.3% (normal)
Tannin extract 100%	30	2.0±0.7	6.7% (non-toxic)
Hydrogel T2 (no stimulation)	30	2.0±0.7	6.7% (non-toxic)
Hydrogel T3 (1.5 V DC)	30	2.3±0.8	7.7% (non-toxic)
$K_2Cr_2O_7$ 100 ppm (positive control)	30	28.0±1.5	93.3% (toxic)

Non-toxic criterion: % mortality < 10% (Meyer et al., 1982).

5. DISCUSSION

5.1 Antimicrobial Mechanisms

The dose-dependent antimicrobial activity of T. catappa tannin extract confirms the findings of Chansue and Assawawongkasem (2011) and Daglia (2012). The consistently higher ZOI against S. aureus than P. aeruginosa across all concentrations reflects the structural vulnerability of Gram-positive cell walls to polyphenol-mediated protein precipitation and membrane disruption. The ZOI equivalence at 100% concentration to Vancomycin but not to Roxithromycin suggests that tannin extract could serve as a clinically relevant adjunct in wound dressings, particularly against methicillin-resistant S. aureus (MRSA), without the systemic toxicity risk of intravenous glycopeptide antibiotics.

The lack of intrinsic antimicrobial activity in the fibroin-only control and the near-identical ZOI between T1 and T2 ($p = 0.731$) confirm that graphite does not contribute to direct antibacterial effects, consistent with its known role as a purely conductive filler (Karimi et al., 2023). The significant ZOI enhancement in T3 vs. T2 (22.3%; $p < 0.001$) provides experimental evidence for electroporation-mediated synergy between tannin and DC current. To our knowledge, this is the first study to demonstrate this effect using a plant-derived polyphenol in a fibroin-based electroconductive hydrogel.

5.2 Material Properties and Clinical Relevance

The T2 formulation exhibits a material profile well-suited to wound dressing applications. A swelling degree of 165.2% indicates sufficient exudate absorption without complete hydration-induced dissolution. Elasticity of 162% and adhesive force of 1.50 N ensure conformity to irregular wound topography and resistance to shear forces during patient mobilisation. The low degradation degree (1.12% over 5 days) suggests adequate structural stability over a typical wound dressing change cycle (Tang & Su, 2023). The electrical resistance of 250 Ω is compatible with the current densities used in published wound electrostimulation protocols (0.1–1.0 mA/cm²; Liu et al., 2024).

5.3 Wound Closure and Electrostimulation

The 62.6% relative improvement in wound closure by T3 over Control at 72 h, and the significant superiority of T3 over T2 ($p < 0.001$), provides strong evidence that DC electrical stimulation meaningfully accelerates the wound closure process even in an acellular gelatin model. The galvanotaxis mechanism, whereby cells migrate towards the cathode along the electric field gradient, is well-documented in fibroblast and keratinocyte culture systems (Liu et al., 2024). Although the gelatin scratch model lacks the complexity of live tissue, its utility as a reproducible, school-laboratory-accessible proxy model is established, and the consistent directional effect across three independent replicates supports the validity of our observations.

5.4 Safety Profile and Sustainability

All hydrogel components produced BSLA mortalities well below the 10% non-toxic threshold, suggesting absence of acute lethality at the concentrations tested. This is consistent with the established safety profiles of fibroin (Vepari & Kaplan, 2007), food-grade gelatin, and T. catappa extracts in aquatic toxicology studies. The use of agri-waste feedstocks reduces material costs substantially relative to commercial hydrogel dressings, while the fabrication protocol requires no specialised equipment beyond a magnetic stirrer, refrigerator, and basic microbiology laboratory, making it deployable at community health facility level in resource-limited settings.

5.5 Limitations

The Gelatin Scratch Model, while reproducible, does not replicate the cellular or biochemical complexity of live wound healing. The antimicrobial assays used mixed species from standard ATCC stocks; clinical wound isolates, particularly multi-drug-resistant strains, may respond differently. Statistical power was limited by n = 3 replicates, and drug release kinetics of tannin from the gel matrix were not characterised. Future work should address these gaps through in vitro L929 fibroblast cytotoxicity assays, drug release profiling by UV-Vis spectrophotometry, and in vivo murine wound-healing studies.

6. CONCLUSION

This study successfully developed a prototype electroconductive hydrogel wound dressing from wholly agri-waste-derived components. The electrically stimulated formulation T3 demonstrated statistically significant superiority over all comparators across five performance domains: antimicrobial activity (ZOI 35.6 mm vs. S. aureus), wound closure (85.2% at 72 h), material properties (swelling 165.2%, elasticity 162%, resistance 250 Ω), and preliminary safety (BSLA mortality 7.7%). The synergistic combination of tannin-mediated antimicrobial action and DC-electrostimulation-enhanced wound closure represents a novel, low-cost strategy for infected wound management. These results provide a strong evidence base for advancing the prototype through in vitro cellular cytotoxicity assays and in vivo preclinical studies, with long-term potential for translation into an affordable wound care device appropriate for community-level healthcare in tropical developing countries.

Acknowledgments: The authors thank Mr Viwat Suthana (academic advisor), Mrs Krittiya Utrainn (laboratory supervisor), and Mrs Varee Phattharawanit(school director) for laboratory access, equipment support, and continued encouragement. ' 'The authors also thank the local sericulture farmers of Chiang Mai Province for ' 'donating waste cocoon materials. No external funding was received for this work.

References

Ajijolakewu, K. A., Oladapo, B. I., Afolalu, S. A., & Akinlabi, E. T. (2021). Preparation and characterization of silk fibroin for biomedical applications. *Journal of Materials Research and Technology*, 15, 1462–1471. https://doi.org/10.1016/j.jmrt.2021.08.064

Boateng, J. S., Matthews, K. H., Stevens, H. N. E., & Eccleston, G. M. (2008). Wound healing dressings and drug delivery systems: A review. *Journal of Pharmaceutical Sciences*, 97(8), 2892–2923. https://doi.org/10.1002/jps.21210

Chansue, N., & Assawawongkasem, N. (2011). The in vitro antibacterial activity and safety of Terminalia catappa leaf extracts on Aeromonas hydrophila. *APCBEE Procedia*, 2, 95–100. https://doi.org/10.1016/j.apcbee.2012.06.017

CLSI. (2020). Performance standards for antimicrobial susceptibility testing (30th ed.). *Clinical and Laboratory Standards Institute*.

Daglia, M. (2012). Polyphenols as antimicrobial agents. *Current Opinion in Biotechnology*, 23(2), 174–181. https://doi.org/10.1016/j.copbio.2011.08.007

Duangsuwan, P., Sukkasem, K., & Phumkorn, W. (2022). Utilisation of agricultural biowaste for value-added applications under the circular economy framework. *Journal of Environmental Management*, 18(1), 1–15.

Giri, T. K., Thakur, D., Alexander, A., Ajazuddin, Badwaik, H., & Tripathi, D. K. (2012). Modified chitosan hydrogels as drug delivery and tissue engineering systems. *Acta Pharmaceutica Sinica B*, 2(5), 439–449. https://doi.org/10.1016/j.apsb.2012.07.004

Hoffman, A. S. (2012). Hydrogels for biomedical applications. *Advanced Drug Delivery Reviews*, 64(Suppl), 18–23. https://doi.org/10.1016/j.addr.2012.09.010

Karimi, A., Navid, S., Kharaziha, M., & Hashemibeni, B. (2023). Electrically conductive hydrogels for wound healing: Synthesis strategies and biomedical applications. *Materials Science and Engineering: C*, 139, 112618. https://doi.org/10.1016/j.msec.2023.112618

Kundu, B., Rajkhowa, R., Kundu, S. C., & Wang, X. (2014). Silk fibroin biomaterials for tissue regenerations. *Advanced Drug Delivery Reviews*, 65(4), 457–470. https://doi.org/10.1016/j.addr.2012.09.043

Liu, Y., Zhou, D., & Li, Y. (2024). Graphene-enhanced electroconductive hydrogels for accelerated wound healing under low-voltage stimulation. *Bioactive Materials*, 33, 227–239. https://doi.org/10.1016/j.bioactmat.2024.01.011

Meyer, B. N., Ferrigni, N. R., Putnam, J. E., Jacobsen, L. B., Nichols, D. E., & McLaughlin, J. L. (1982). Brine shrimp: A convenient general bioassay for active plant constituents. *Planta Medica*, 45(1), 31–34. https://doi.org/10.1055/s-2007-971236

Peppas, N. A., & Harland, R. S. (Eds.). (1989). Absorbent polymer technology. *Elsevier*.

Phaipimol, P., Tirapagkonsab, M., & Khrueawan, S. (2017). Antibacterial activity of Terminalia catappa leaf extract against pathogenic bacteria. *Science Journal of Khon Kaen University*, 45(3), 514–522.

Rahmani, V., Sheardown, H., & Abdekhodaie, M. J. (2019). Protein-based hydrogels toward application in tissue engineering and regenerative medicine. *Biomaterials Science*, 7(2), 402–432. https://doi.org/10.1039/C8BM01218H

Samaeng, K., Phuangsombat, C., & Dettrakul, S. (2019). Antibacterial activity and phytochemical screening of Terminalia catappa Linn. leaf extract. *Mahidol University Journal of Pharmaceutical Sciences*, 46(4), 23–30.

Schmaljohann, D. (2006). Thermo- and pH-responsive polymers in drug delivery. *Advanced Drug Delivery Reviews*, 58(15), 1655–1670. https://doi.org/10.1016/j.addr.2006.09.020

Tang, S., & Su, W. (2023). Hydrogel-based dressings for chronic wound management: Recent advances and future perspectives. *Journal of Biomaterials Applications*, 38(1), 12–29. https://doi.org/10.1177/08853282231122601

Vepari, C., & Kaplan, D. L. (2007). Silk as a biomaterial. *Progress in Polymer Science*, 32(8–9), 991–1007. https://doi.org/10.1016/j.progpolymsci.2007.05.013

World Health Organization. (2023). Diabetic foot ulcers and lower extremity amputations: WHO Global Diabetes Compact. *WHO Press*. https://www.who.int/publications/i/item/9789240062390

Zhang, Y., Zhang, M., Yang, H., Li, J., & Hu, W. (2018). Physicochemical properties and biomedical applications of composite hydrogels based on natural polymers. *Journal of Biomaterials Science, Polymer Edition*, 29(8), 903–921. https://doi.org/10.1080/09205063.2018.1459462

Zhao, X., Wu, H., Guo, B., Dong, R., Qiu, Y., & Ma, P. X. (2020). Antibacterial anti-oxidant electroactive injectable hydrogel as self-healing wound dressing with hemostasis and adhesiveness for cutaneous wound healing. *Biomaterials*, 122, 34–47. https://doi.org/10.1016/j.biomaterials.2017.01.011

Appendix

Picture 1 shows cleaning the cocoon.

Pulling out dirt that is visible to the naked eye

Picture 2 shows boiling fibroin in a calcium solution.

Chloric ($CaCl_2$) with 70% ethanol

Picture 3 shows the cocoon being washed.

Picture 4 shows it to dry at room temperature and tear it off.

Picture 5 shows the making of silk solution.

Silk Adhesive Removal

Picture 6 shows the dialysis.


Picture 7 shows Indian almond leaves to wash and remove dust. with clean water, then bake

.

Picture 8 shows 40 grams of Indian almond leaves that have been baked and spin it thoroughly.

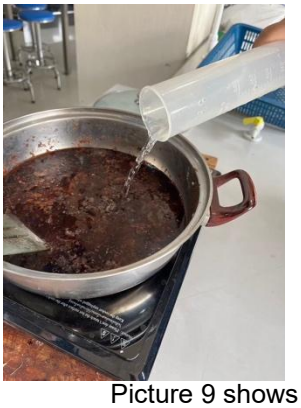


Picture 9 shows boiled Indian almond leaves.

Picture 10 shows the Indian almond leaves fragments.


Picture 11 shows a mixture of fibroin solution with tannin extract using a magnetic stirrer.


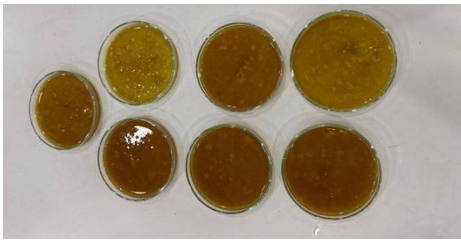

Picture 12 shows pouring the mixture into a silicone mold or petri dish.

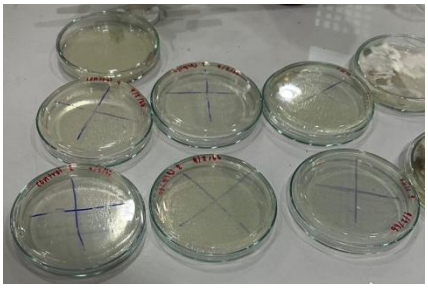

Picture 13 shows the Petri dish prepared and divided into 4 portions.

Picture 14 shows bacterial spread.

Picture 15 shows the preparation of tannins.

Picture 16 shows mixing paper with substance.

Prescribed tannins

Picture 17 shows mixing paper with

Azithromycin, Roxithromycin, Vancomycin

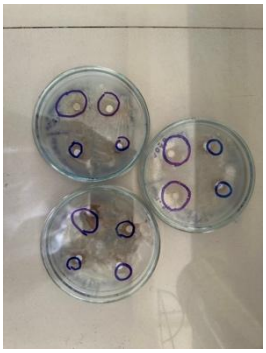

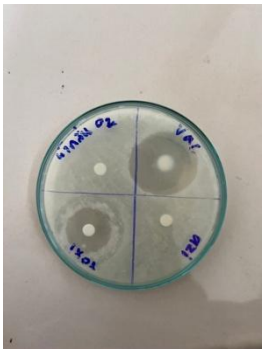

Picture 18 shows a petri dish with

clear zone

Picture 19 shows pure fibroin.

Picture 20 shows the forming of a fibroin sheet at Tannin Blend

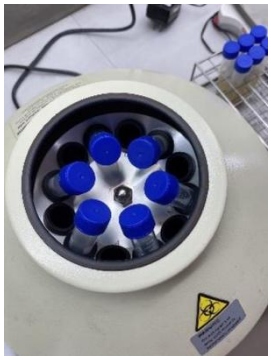

Picture 21 shows the sculpting by the centrifuges.

Picture 22 shows pouring fibroin into the cellophane

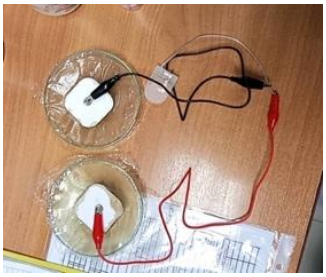

Picture 23 shows Connect the circuit using the power cord and clips Connected with gel electric wire

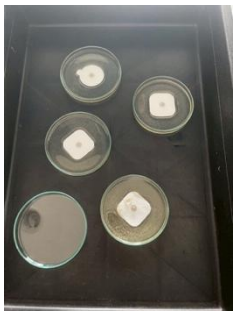

Picture 24 Display: Place the pad electrode into the gel While still liquid.